BACCHUS

Impact of Biogenic versus Anthropogenic emissions on Clouds and Climate: towards a Holistic UnderStanding

Collaborative Project

SEVENTH FRAMEWORK PROGRAMME
ENV.2013.6.1-2

Atmospheric processes, eco-systems and climate change

Grant agreement no: 603445

Deliverable number:	**D2.2**
Deliverable name:	Parameterisations of the impact of aerosol origin (natural versus anthropogenic) and chemistry (organic aerosol formation and aerosol ageing) in CCN and IN and associated uncertainties estimate
WP number:	2
Delivery date:	Project month 30 (31/05/2016)
Actual date of submission:	07/06/2016
Dissemination level:	PU
Lead beneficiary:	PSI
Responsible scientist/ administrator:	
Estimated effort (PM):	64
Contributor(s):	Julia Yvonne Schmale, Martin Gysel Beer, Urs Baltensperger (PSI); Matteo Rinaldi, Stefano Decesari (CNR); Matthew Crooks, Paul Connolly, David Topping, Gordon McFiggans (UMAN); Ken Carslaw (ULEEDS); Yvonne Boose, Berko Sierau, Ulrike Lohmann (ETHZ); Giorgos Fanourgakis, Stelios Myriokefalitakis,
Estimated effort contributor(s) (PM):	Total: 64 PSI:18 PM; CNR: 6 PM; UMAN:20 PM; UOC: 20PM
Internal reviewer:	Maria Kanakidou

Executive summary

This deliverable is related to Question 1b of the project: '*What is the relative impact of anthropogenic versus natural aerosols on liquid, mixed-phase and ice clouds (CCN versus IN) in various environments, and/or climate regimes? What is the contribution of the biogenic aerosol as compared to the other natural aerosol types (dust, sea salt) on aerosol-cloud interactions?*'

In particular, the work summarized in this deliverable aims to improve the organic aerosol (OA) representation in the models accounting for all major identified processes of OA formation and transformation in the atmosphere; to develop parameterizations of formation and growth of cloud condensation nuclei (CCN) and ice nuclei (IN) and ageing of aerosols by atmospheric chemical and dynamic processing. Focus is put on understanding aerosol ageing in the atmosphere and its influence on CCN properties using model simulations and statistical analyses of observations. Gas-phase, heterogeneous and aqueous/multiphase atmospheric chemistry of organics are considered.

Simplified parameterizations are developed and tested to investigate the impact of aerosol origin (natural versus anthropogenic) and chemistry (organic aerosol formation and aerosol ageing) in CCN and IN, and sensitivity modelling studies are performed to estimate the associated uncertainties. In this respect, the performed work that is here reported concerns: i) the study of the effects of aerosol size, composition and semi-volatile organic compounds (SVOCs) on CCN activation and warm rain using data from WP1 and a detailed process model, comparing natural versus anthropogenic conditions; ii) the analysis of the particle mixing state (internal vs. external mixtures) iii) CCN 'closure' studies of observed CCN concentrations and size distributions; (iv) study of marine OA and dust as IN; (v) study of the uncertainty in the simulated global CCN concentrations due to uncertainties in simulated OA.

Contents

Summary of results

1. Effects of aerosol size, composition and semi-volatile organic compounds (SVOCs) on CCN activation

1.1. Parameterization of co-condensation of SVOC into multiple aerosol particle modes

Abstract. An existing equilibrium partitioning model for calculating the equilibrium gas/particle concentrations of multiple semi-volatile organics within a bulk aerosol is extended to allow for multiple non-volatile aerosol modes of different sizes and chemical compositions. In the bulk aerosol problem the partitioning coefficient determines the fraction of the total concentration of semi-volatile material that is in the condensed phase on the aerosol. This work modifies this definition for multiple polydisperse aerosol modes to account for multiple condensed concentrations; one for each semi-volatile on each non-volatile aerosol mode. The pivotal assumption in this work is that each aerosol mode contains a non-volatile constituent thus overcoming the potential problem of smaller particles evaporating completely and then condensing on the larger particles to create a monodisperse aerosol at equilibrium. The resulting coupled non-linear system is approximated by a simpler set of equations in which the organic mole fraction in the partitioning coefficient is set to be the same across all modes. By perturbing the condensed masses about this approximate solution a correction term is derived which accounts for much of the removed complexities. This method offers a greatly increased efficiency in calculating the solution without significant loss in accuracy, thus making it suitable for inclusion in large scale models.

Overview and Key Results. This BACCHUS study by Crooks et al. (2016) derives and presents the equations for equilibrium partitioning of SVOCs between a vapour phase and condensed phases spread across multiple modes of different sizes and chemical composition. The form of the equations is such that direct numerical solvers cannot reliably calculate the solution, especially in useful time frames. To overcome this, two parameterizations are presented that approximate the solution. The first assumes a constant mole fraction of SVOCs across all particle modes and the second one uses in addition a correction term to improve the accuracy.

Many simulations with random parameter values have been run and the solutions calculated using the two approximations, with and without the correction term, are compared against the solution from a numerical solver using the first approximation as an initial guess. Figure 1 shows the accuracy in the organic mass fraction from the two approximations. Overall, the approximations perform well but the addition of the correction term improves the accuracy significantly at relative humidities below 100%.

The equations are derived assuming multiple monodisperse particle modes. We study the effects of relaxing this assumption to model multiple lognormal size distributions of particles. It is found that if the median diameters are above about 50 nm then the partitioning equations calculate equilibrium to a very high degree of accuracy when compared to a dynamic condensation model. This is shown in Figure 2. The paper by Crooks et al.(2016) has undergone peer review and is awaiting a response on publication in GMD.

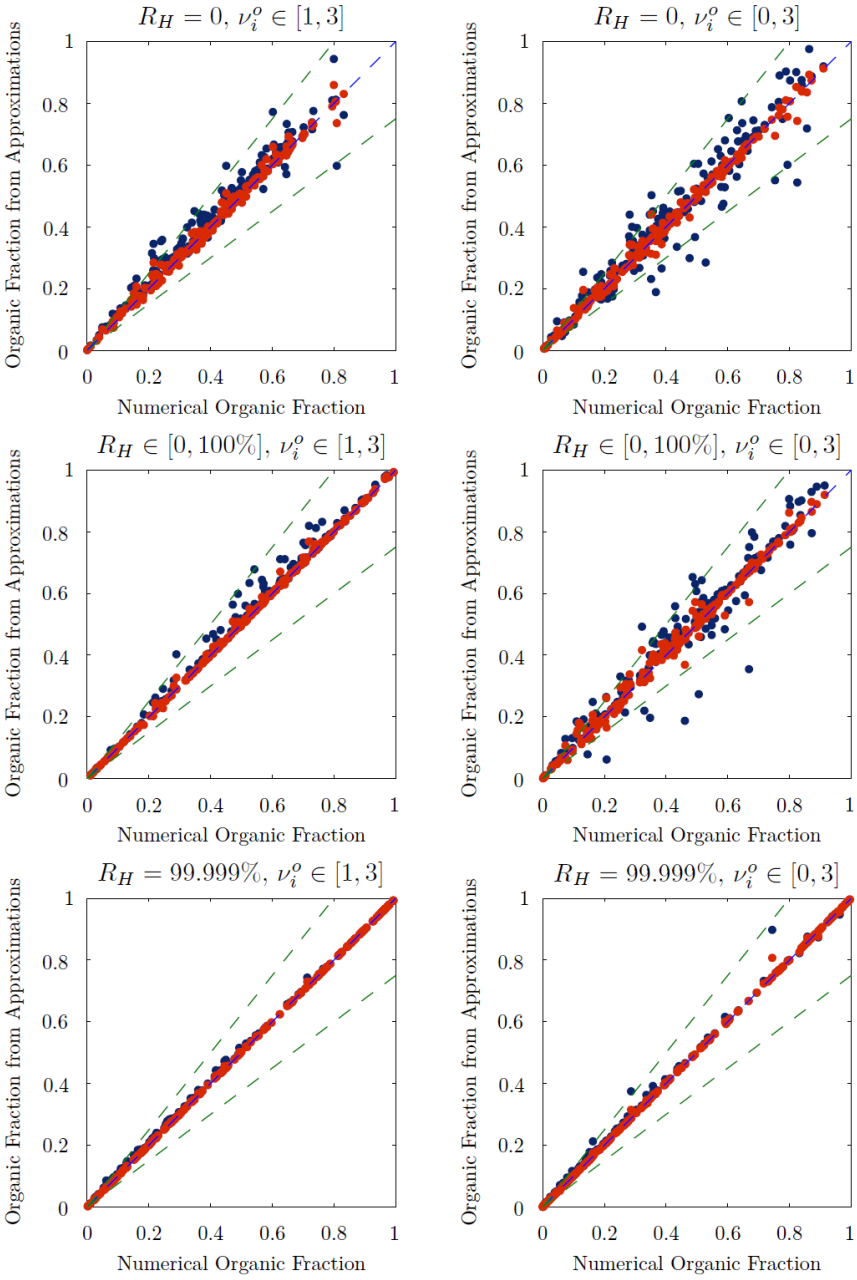

Figure 1. Comparison of the organic mass fraction from the two approximations against that calculated using the non-linear solver for randomly chosen parameters. The solution is calculated for 2 to 6 modes and only the mass fraction of the first is plotted. The constant mole fraction solution is shown in blue and the red dots show the effect of the additional correction term. 25% error margins are shown by the dashed green lines.

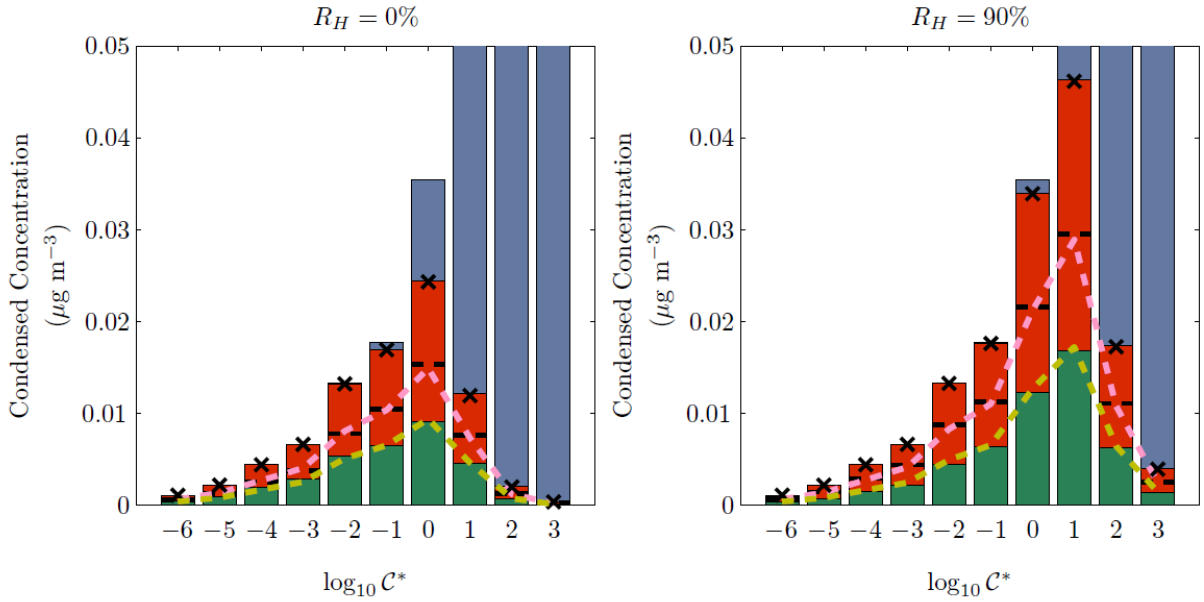

Figure 2. Stacked bar charts show the condensed mass in each volatility bin from the dynamic condensation model on the smaller (green) and larger (red) modes of ammonium sulphate. The height of the red region only is shown by the horizontal dashed black lines. The median diameters of the modes are 50 nm and 125 nm. Equivalent values from the equilibrium partitioning theory are shown by the yellow and pink dashed lines.

Parameterisation on the Effects of SVOCs on Cloud Droplet Number

Further work has been carried out to create a parameterisation that can calculate the number of cloud droplets that result from multiple lognormal aerosol particle modes, and which includes the effects of SVOCs. Early results were presented at EGU 2016 in both a poster and an oral presentation (see D5.5, http://www.bacchus-env.eu/public/Deliverables/D5.5_month30_final.pdf), and a paper is being prepared that will be submitted in the coming weeks. A review of the work is presented here.

The parameterisation is based on the same model as described in Connolly et al. (2014), which solved the problem for a single lognormal size distribution of particles. At cloud base, almost all of the SVOCs are in the condensed phase as a result of the elevated relative humidity (RH). The difficulty, however, is ascertaining how this condensed mass is spread between the different modes. This is important as the additional aerosol mass from the condensed SVOCs increases particle sizes and subsequently affects the number of cloud droplets.

We have developed a new parameterisation for use with multiple modes, which approximates the solution to the dynamic condensation of the SVOCs near cloud base. In the governing equations we have neglected changes in the diameter, pressure and temperature in order to simplify the equations. This, together with the assumption that the equilibrium vapour pressure of the organic compounds is negligible when RH is near 100%, allows obtaining an analytic solution of the form

$$y = at + be^{-ct}$$

Here y is the condensed mass of an organic compound, t is time and a, b, and c are parameters that depend on the initial temperature, pressure, RH and diameter of the aerosol particles. By evaluating this equation at 100% RH we calculate the additional aerosol mass on each mode and change the median diameter and geometric standard deviation in the lognormal size distributions in such a way as to conserve mass and maintain constant arithmetic standard deviations,

$$SD = e^{lnd_m + \frac{1}{2}ln^2\sigma}\sqrt{e^{ln^2\sigma} - 1}$$

of each mode. Here d_m and ln σ are the median diameter and geometric standard deviation, respectively. These new size distributions and chemical compositions are then used in the Fountoukis and Nenes (2005) parameterisation for cloud droplet activation.

The parameterisation has been tested using 3 lognormal aerosol particle modes with size distributions given by Van Dingenen et al. (2004). Examples of anthropogenic and biogenic SVOC emissions from the literature (Cappa and Jimenez, 2010; Hermansson et al., 2014) are also used. Results for the Natural and Near-City environments from Van Dingenen et al. (2004) are calculated using the anthropogenic and biogenic SVOC volatility distributions, respectively, and are shown in Figures 3 and 4. Note that Van Dingenen et al. (2004) classify as Near-City Environment the anthropogenically influenced background at a distance from large pollution sources of about 3–10km, while at a distance of more than 50 km the environment is characterized as Natural background. Total SVOC concentrations are here rescaled so that at 90% RH the condensed mass makes up a given organic mass fraction of aerosol particles. Results from the parameterisation are compared against a parcel model.

With the **Natural environment conditions** (Fig. 3) the parameterisation performs outstandingly at all concentrations and updraft velocities. Even at very high concentrations (Fig. 3c) the agreement is good with a slight over prediction in the parameterisation at high updrafts. In the majority of cases including SVOCs acts to increase the number of cloud drops. At very high concentrations, however, SVOCs suppress the number concentration compared to only condensing water. This is due to the largest particles growing so large with the condensing SVOCS that they suppress the supersaturation and prevent smaller particles from activating. The parameterisation also captures this suppression.

In the **Near-City environment** there are, overall, far fewer particles activating due to the smaller sizes of the aerosol modes. At the lower SVOC concentrations (Fig. 4a,b, for 10% and 50% organic mass fraction, respectively) the agreement between the parcel model and the parameterisation is very good but, like in the Natural environment, there is some discrepancy at the higher concentrations (Fig. 4c, for 90% organic mass fraction). In both cases, however, the 90% mass fraction is chosen to try to test the parameterisation under wide parameter space since this aerosol organic mass fraction is close to the upper end of the respective observations. In this high

concentration case, the parameterisation under predicts the fraction of aerosols that activate into cloud droplets compared to the parcel model at low updrafts but the number of cloud drops is still small in both cases. At higher updrafts the parameterisation predicts a suppression effect in cloud droplet number from the SVOCs whereas the parcel model sees an enhancement.

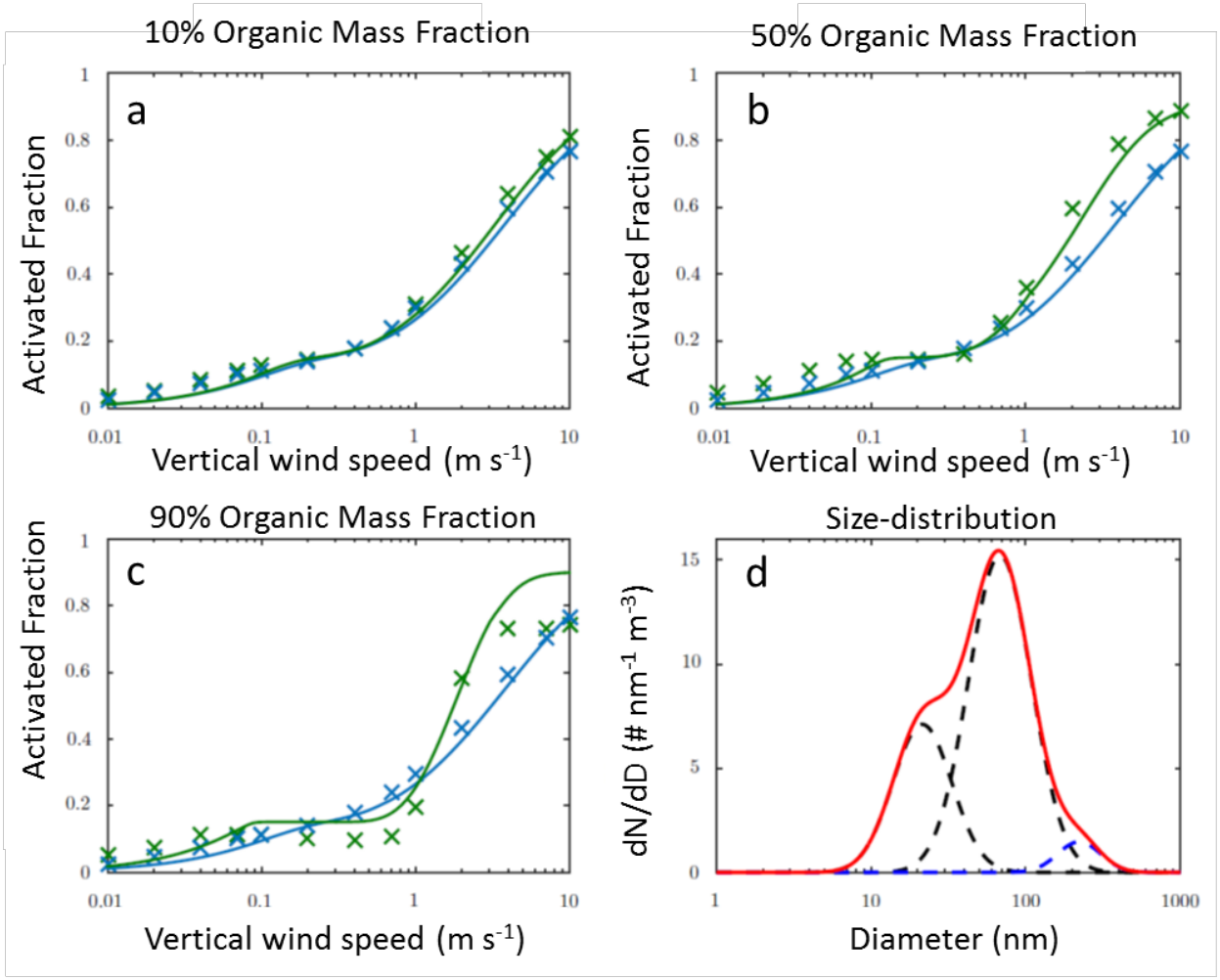

Figure 3. Fraction of aerosol particles that activate into cloud droplets as a function of vertical updraft for different SVOC concentrations with organic mass fractions of (a) 10%, (b) 50%, (c) 90%. (d) Aerosol size distributions from the **Natural environment**.. Parcel model simulations with and without SVOCS are shown by the green and blue crosses, respectively. The solid lines show the analogous quantities from the parameterisation.

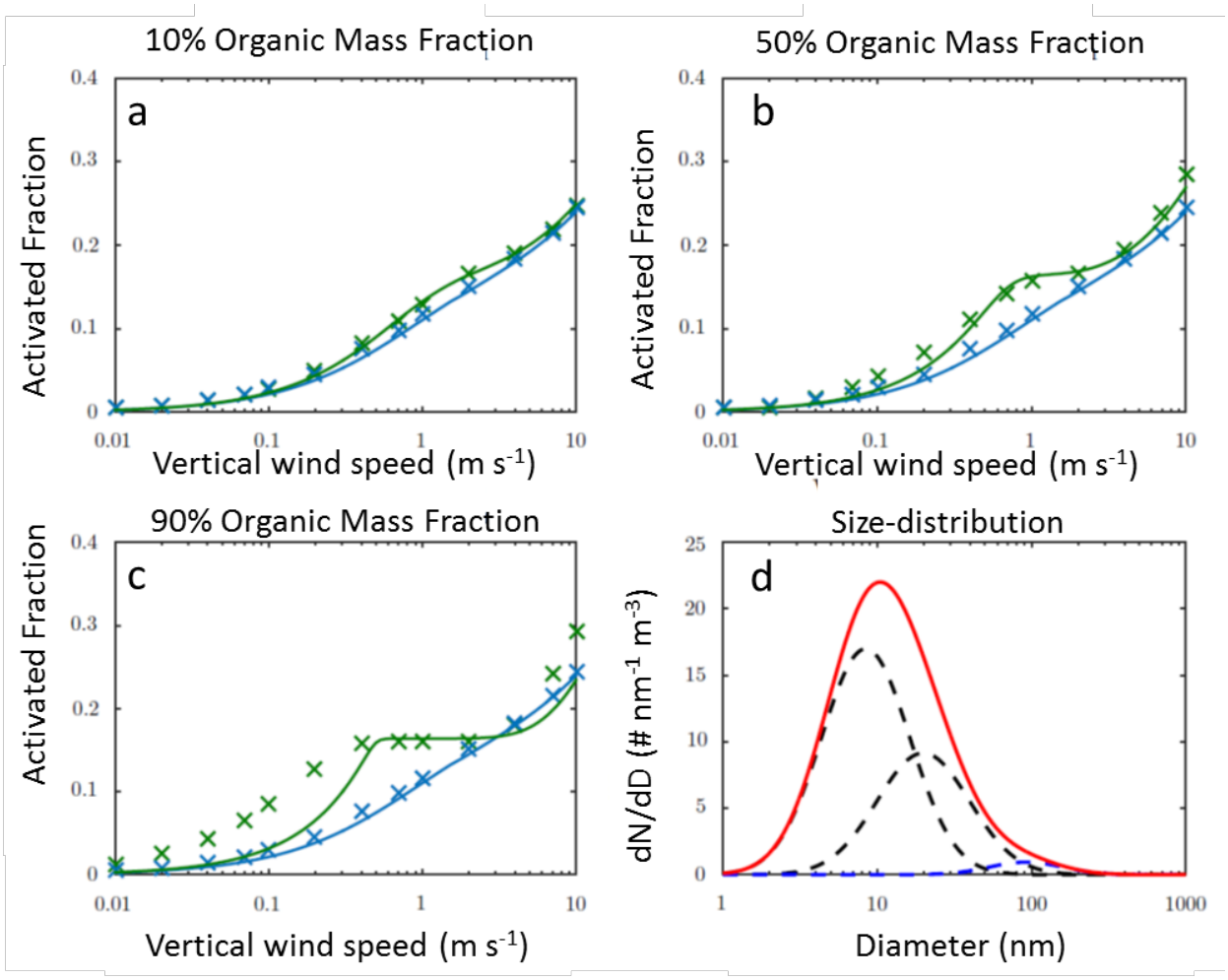

Figure 4. Fraction of aerosol particles that activate into cloud droplets as a function of vertical updraft for different SVOC concentrations with organic mass fractions of (a) 10%, (b) 50%), (c) 90%. (d) Aerosol size distributions from the **Near-City (Anthropogenic) environment**. Parcel model simulations with and without SVOCS are shown by the green and blue crosses, respectively. The solid lines show the analogous quantities from the parameterisation.

1.2. Observational dataset and analysis

Time series of at least one year duration for aerosol size distribution, chemical composition and CCN number concentrations are obtained from six stations that represent different environments and are listed in Table 1.

These data have been analyzed with regard to their seasonal variability and Fig. 5 provides an overview of the data in form of seasonal cycles. In brief, panel a) shows the CCN number concentrations at a supersaturation of 0.2 % that reflect expected features associated with the dominant meteorological and chemical conditions in the different environments. For example, at the ATTO tower (ATT) concentrations are lower during the rainy season in the beginning of the year than during the dry season. At Jungfraujoch (JFJ), concentrations peak in summer due to boundary layer air mass uplift.

Table 1: List of stations from where data sets were obtained

Station Name	Abbreviation	Environment	Time period
ATTO tower	ATT	Brazil, rain forest	Mar 2014 – Feb 2015
CESAR tower, Cabauw	CES	The Netherlands, rural-remote, coastal influence	2012 – 2014
Jungfraujoch	JFJ	Switzerland, high alpine	2012 – 2014
Melpitz	MEL	Germany, rural-remote	2012 – 2014
Mace Head	MHD	Ireland, coastal	2011 – 2013
Smear station II, Hyytiälä	SMR	Finland, boreal forest	2012 – 2014

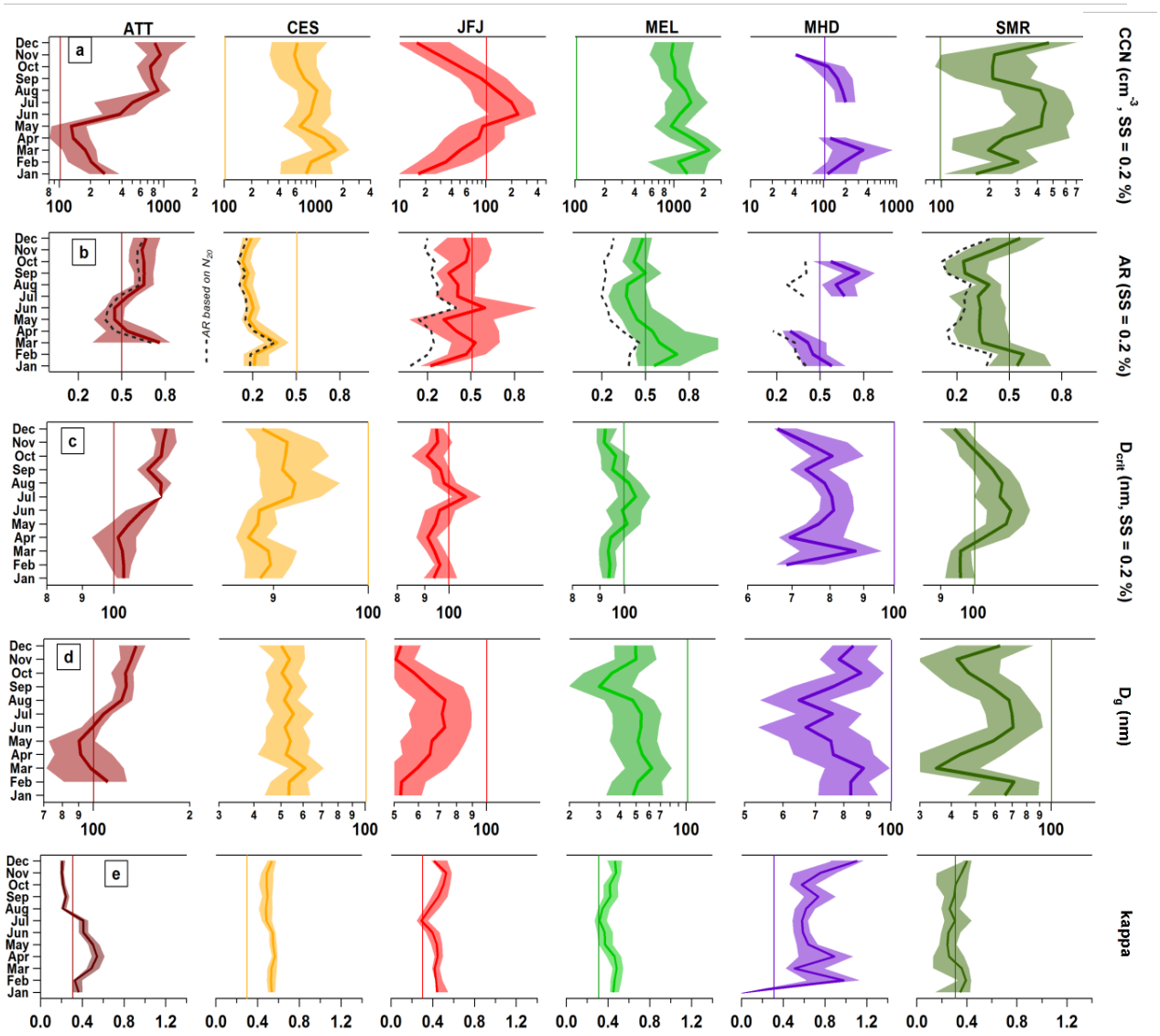

Figure 5. Seasonal cycles of a) CCN number concentrations, b) activation ratio based on particle diameters > 50 nm (N_{50}), and N_{20} as dashed lines, c) the critical diameter, d) the geometric mean diameter of N_{20}, e) the hygroscopicity parameter kappa. The reference supersaturation is 0.2 %. The lines indicate median values, the shaded areas represent the inter-quartile range. The vertical colored bars are placed in the same location in each panel at each station for quick data comparability.

Activation ratios (AR) on the basis of particle number concentrations > 50 and 20 nm, critical diameters (D_{crit}) and geometric mean diameters (D_g) (panels b), c) and d) respectively) indicate the role of particle size for CCN number concentrations at the various locations.

On average, particles in the rain forest are larger during the dry season than at other sites. They also present larger critical diameter (D_{crit}) than at other sites. Nevertheless, the activation ratio also increases during the dry season at the ATT site compared to the wet season.

In the boreal forest (SMR), the relation between particle size and activation ratio is different. Particles are largest in summer and winter; however, the activation ratio is lowest in summer due to the high critical diameter, while in winter the activation ratio peaks. This is an indication for the importance of the chemical composition of the particles.

Similarly, the activation ratio at JFJ does not peak in summer, when particles are largest.

1.3. Hygroscopicity parameter and influence of organic aerosol mass

The chemical composition of particles is reflected by the hygroscopicity parameter kappa (κ) in Fig. 5 panel e). The overall κ, including organic and inorganic components, is calculated based on the mixing rule as given by (Petters and Kreidenweis, 2007):

$$\kappa = \sum_i \varepsilon_i \kappa_i$$

with ε = dry component volume fraction.

Values of κ for organic components are assumed to be 0.10 (e.g., Dusek et al., 2006) and for black carbon 0.00 (e.g., Rose et al., 2010).

The κ of inorganic components are calculated based on the following steps:

- assuming κ = 0.3, SS = 0.5 %, T = 5°C, the surface tension of water = 0.0072 J/m a growth factor is derived from which the water activity a_w = 0.9975 is determined
- based on the a_w growth factors for the inorganic component mixtures are calculated using the E-AIM II model (http://www.aim.env.uea.ac.uk/aim/model2/)
- from these growth factors κ as shown in Table 2 is derived.

Fig. 5 panel e) shows the seasonal cycles of κ_1 values (Table 3 first line). To give just one example of the role of κ: For the boreal forest environment (SMR) the particle hygroscopicity is relatively constant over all seasons but winter, when it is higher. This explains why the activation ratio increases in winter when particles are large and κ relatively high in contrast to summer when particles are also large but κ is lower.

Table 2: ***Calculated component κ vs values from ref. [2]***

Component	calculated	from Ref.
H_2SO_4	0.83	0.90 [2]
$(NH_4)_2SO_4$	0.72	0.61 [2]
NH_4NO_3	0.78	0.67 [2]
NH_4HSO_4	0.74	0.91 [2]
NaCl	1.31	1.28 [2]
Organics	0.10*)	0.10 [3,4]
BC	0.00*)	0.01 [5]

*) κ was assumed (not calculated) to be 0.10 for organics and 0.00 for black carbon based on given references.

Table 3: ***Medians of 5 types of total κ for each station based on different assumptions of aerosol chemical composition***

	ATT	**CES**	**JFJ**	**MEL**	**MHD**	**SMR**
κ_1 : all inorganic components, organics, no BC	0.26	0.52	0.41	0.43	0.63	0.30
κ_2 : only $(NH_4)_2SO_4$, NH_4NO_3, organics, no BC	0.21	0.50	0.31	0.42	0.63	0.29
κ_3: Like 1 but with BC	0.25	0.50	0.39	0.42	0.61	0.27
κ_4: Like 2 but with BC	0.20	0.48	0.29	0.42	0.61	0.25
κ_5	0.30	0.30	0.30	0.30	0.30	0.30

For a better comparability of **κ values in the different environments**, Fig. 6 shows box and whiskers plots over the entire data sets of each station. Particle hygroscopicity is similar in the forest environments exhibiting the lowest median values (0.3). At the mountain site as well as the remote-rural / continental site κ values are slightly higher with 0.4, followed by the remote-rural /coastal site where the sea salt influence increases κ values slightly. The highest particle hygroscopicity is measured at the remote coastal site (> 0.6 median value). Note that the hygroscopicity parameter is based on the data obtained by aerosol mass spectrometers, which introduce a bias towards larger particles due to the lower cut-off size of around 100 nm (and 50 nm for MHD). For this reason, κ values in this study are higher than in other studies that used more direct measurements.

Further, the relationship between κ values and the ratio of organic to inorganic aerosol components is explored, see Fig. 7. The average relationship can be described as:

$$\kappa = y_0 + A^{(-\tau * x)}, \text{ with } y_0 = 0.16, \text{ A} = 0.40, \tau = 0.66$$

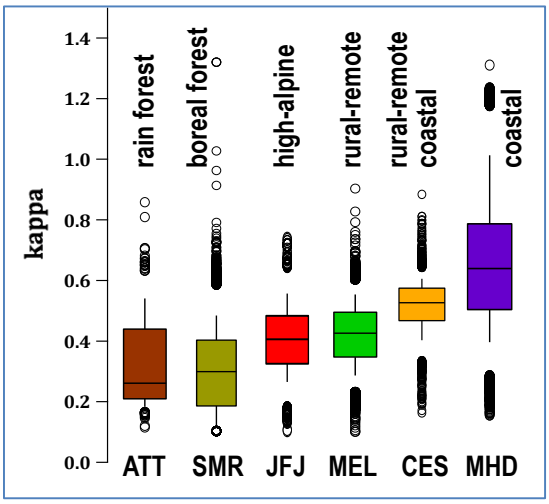

Figure 6. Box plots of κ_1 values for each station. The boxes with the horizontal bar reflect medians and the interquartile range, the whiskers the 10th and 90th percentiles, and the markers the values from the 2.5 and 97.5th percentiles.

The JFJ and MEL data are most representative of the average relation of κ values to the ratio of organic (OA)/inorganic particle. **The aerosol hygroscopicity (κ) is found to be reduced with increasing contribution of OA.**

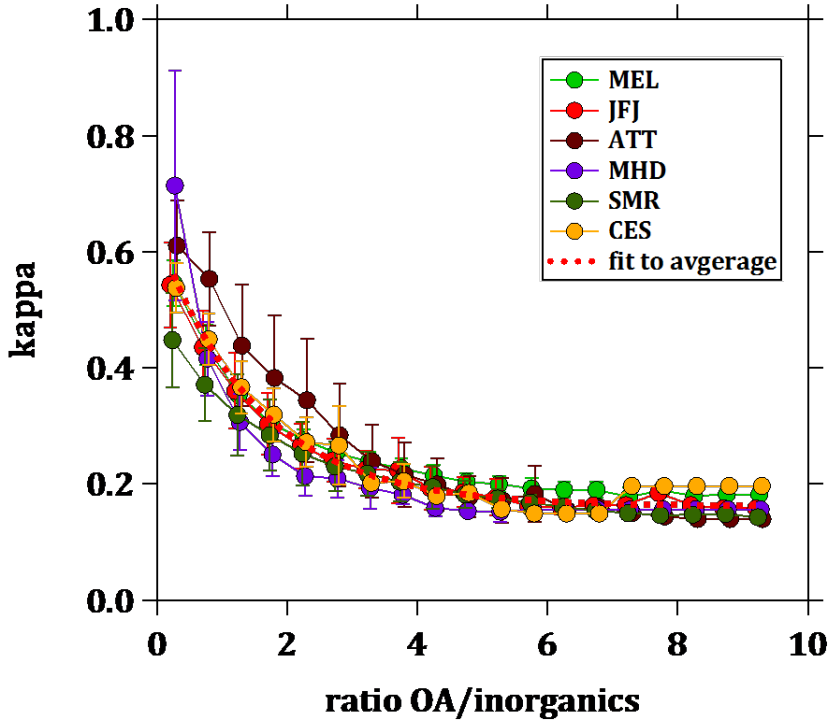

Figure 7. κ_1 values vs ratio of organic to inorganic aerosol. The dashed red line indicates the fit as described in the text.

2. Analysis of the particle mixing state (internal vs. external mixtures)

In addition to the influence of organic aerosol on the κ values, the direct relationship between CCN number concentration and organic aerosol mass can be explored. Fig. 8 shows the scatter plots of the organic and inorganic aerosol mass versus the CCN number concentrations and their linear fits. The correlation between OA mass and CCN number concentration varies across sites. In the forest environments (SMR, ATT), correlation is highest, while at the remote-rural site (MEL) correlation is low. In location with well-mixed particles (JFJ) there is no difference in the slope of the correlations with organic or inorganic aerosol mass, opposed to locations with occasionally externally-mixed particles and local sources (e.g. CES, MHD).

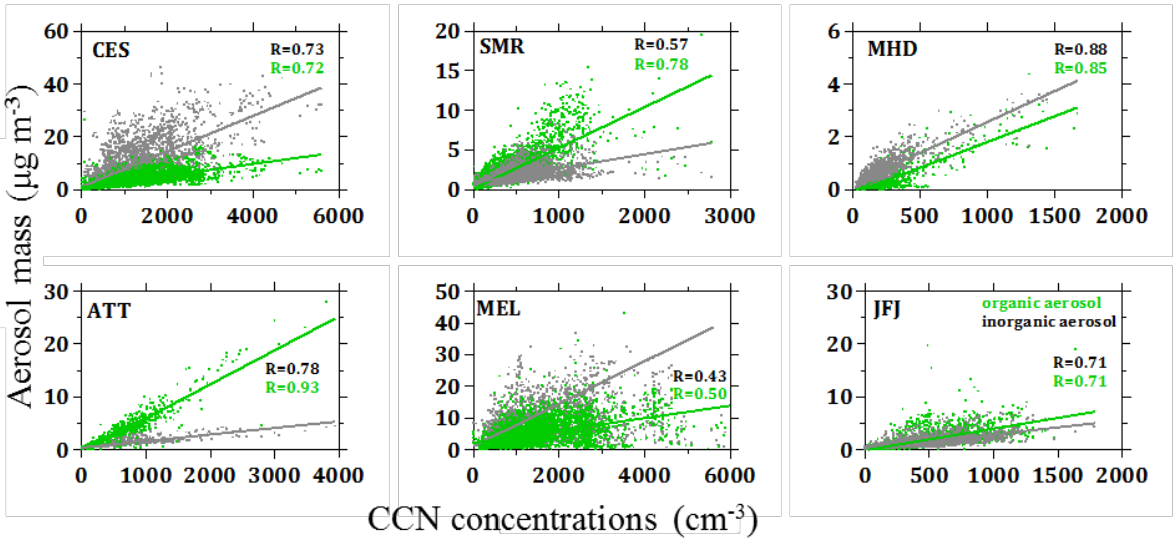

Figure 8. Organic (green) and inorganic (grey) aerosol mass vs CCN number concentration at 0.5 % SS at each station, the Pearson correlation coefficients (R) are given for both species.

3. CCN closure studies of observed CCN concentrations and size distributions

CCN number concentrations can be predicted by the κ-Köhler theory (Petters and Kreidenweis, 2007):

$$S(D) = \frac{D^3 - D_d^3}{D^3 - D_d^3(1-\kappa)} \exp\left(\frac{4\sigma_{s/a} M_w}{RT\rho_w D}\right)$$

with S = saturation ratio, D = droplet diameter, D_d = dry diameter, σ_s = surface tension of water, M_w = molecular weight of water, ρ_w = density of water, R = universal gas constant and T = temperature.

Results of the closure are shown in Fig. 9a. Calculations were carried out with the five different κ values as presented in Table 3 to test the sensitivity of the prediction to the calculated particle hygroscopicity. Generally, predicted and measured CCN concentrations agree within ± 20 % for

the stations MHD, MEL, ATT and SMR as reflected by the slope of the fit to the predicted versus measured data. Results within this range are expected as the measurement uncertainty is roughly in the same range with 10 % for both CCN and particle counters. Results for JFJ and CES are outside this range which reflects higher uncertainty in the particle and CCN counting rather than the use of an inappropriate κ value. This conclusion is derived from a sensitivity study conducted on the JFJ data (see Fig. 10), where parameters entering the κ –Köhler equation were varied. κ values would have to be unrealistically high or low to explain an under- or over-prediction of CCN as obtained for the two stations. The spread of results for each station based on the application of the five κ values shows as well that different assumptions in the aerosol chemical composition as tested here would have only a minor influence on the result. The correlation coefficients (left axis in Fig. 9) indicate how well the observed variability of CCN number concentrations over time is captured by the predictive method. Results show that this works generally well. For MEL the correlation is lower which might be associated to the difference in time resolution of CCN number concentration, chemical composition and size distribution data.

In contrast to the hygroscopicity parameter, **information on the particle size and number concentration can influence the outcome of the prediction much more severely**. Fig. 9b shows the difference of the closure outcome for the default input (κ_1-values, particle number and size distribution data as measured, red symbols) compared to keeping κ-values fixed at 0.3 (grey symbols), to keeping the shape of the size distribution fixed to the average of the data set (green symbols) and to fixing the particle number concentration to each station's median value (black symbols). Fig. 11 shows the details behind the results for MHD as an example.

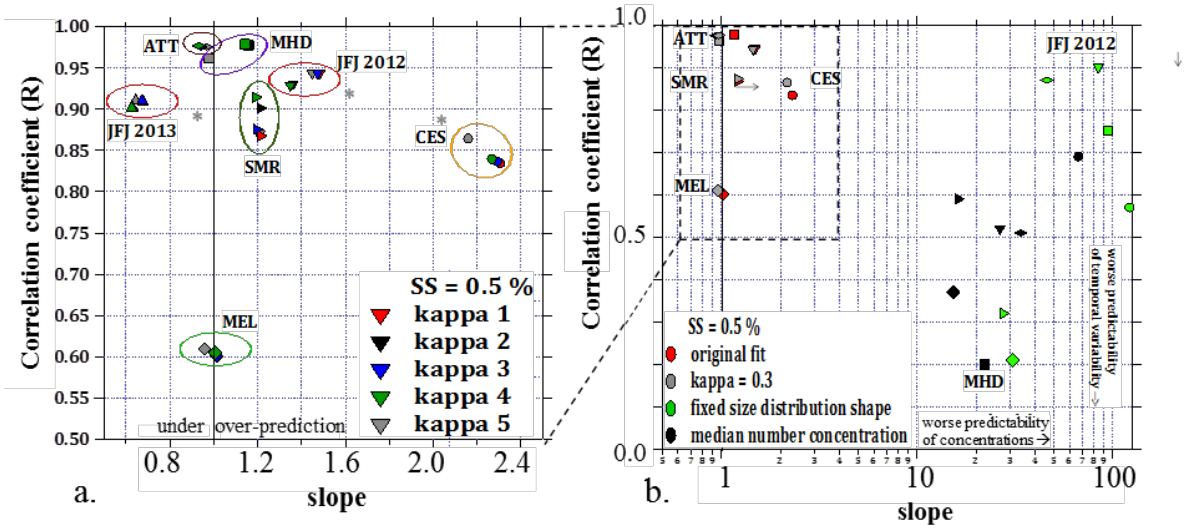

Figure 9. (a) Slope and correlation of predicted vs measured CCN number concentrations for all stations and 5 different kappa values (Table 3). (b) Influence of number concentration, size distribution shape, and chemical composition for predicting CCN concentrations. The different markers represent stations. Red shows the original fit statistics (see text) and grey is derived with kappa value equal to 0.3. Green represents the case where the average size distribution shape of the entire data set was used instead of the actual shape variable with time. Black shows results for when the median particle number concentration at each site was applied instead of the actual temporal variability.

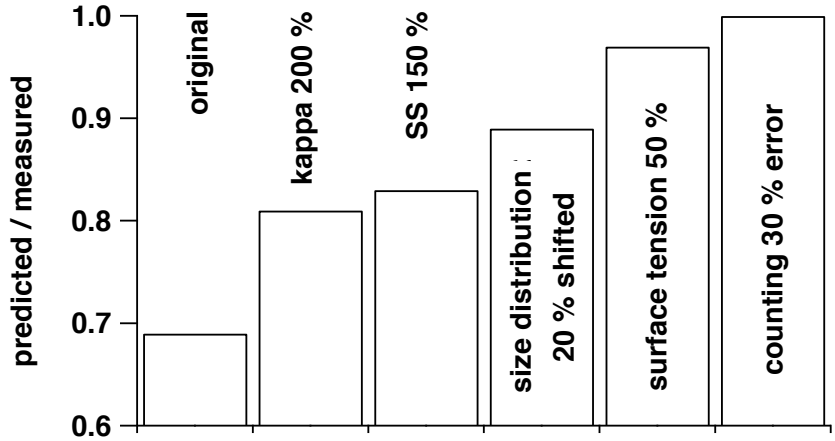

Figure 10. Example for the JFJ station, 2013 (from Fig. 5): sensitivity of predicted vs measured results when varying different parameters of the **κ**-Köhler equation.

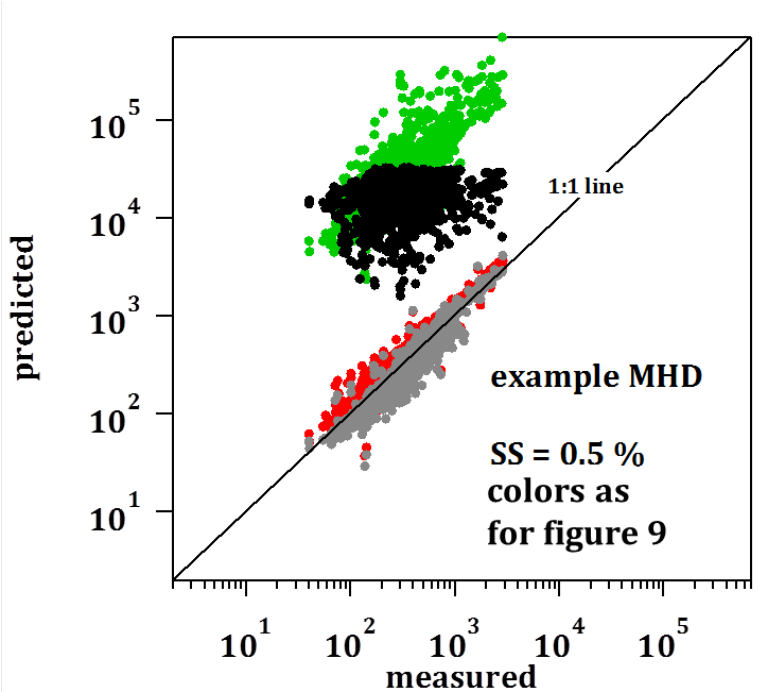

Figure 11. Example of a closure sensitivity study for MHD (CCN number concentrations). Red dots represent the default closure parameters (see text). Grey dots show the case where κ-values were fixed to 0.3, green dots represent the case where the size distribution shape is invariable, and black dots show the result for keeping the particle number concentration fixed.

4. Marine organic aerosols and dust as IN particles.

Boose et al. (2016) studied the ice nucleation ability of desert dust on samples collected after airborne transport in the troposphere from Sahara to different locations. They found that a higher

IN activity in a given sample can be attributed to the K-feldspar content in the sample (at T>250K) while at lower temperatures (238-245 K) it is attributed to the sum of feldspar and quartz content of the sample. They have also compared their data to an existing desert dust parameterisation for use in climate models (Table 4, from Boose et al., 2016) and suggested that for an improved prediction of the IN ability of desert dust in the atmosphere, emissions of feldspar and quartz minerals have to be explicitly considered in the models.

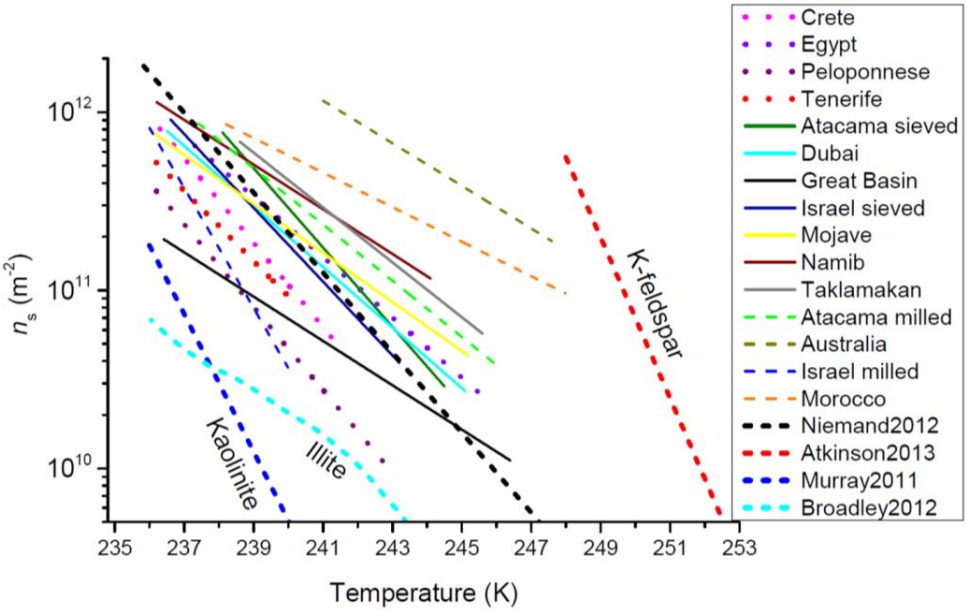

Figure 12. Ice-active surface site density fits of all dust samples. The fit parameters are given in Table 4. Solid lines indicate surface-collected and sieved samples, dashed lines surface-collected and milled samples and dotted lines airborne samples. Parameterisations for desert dust (Niemand et al., 2012), kaolinite (Murray et al., 2011) and k-feldspar (Atkinson et al., 2013).

Table 4. Overview of the dust n_s fit parameters a and b, the resulting R^2 and the number of data points in each fit, N.

Collection site	type	a (K^{-1})	b	R^2	N
Atacama	sieved	0.513	9.39	0.91	36
Atacama	milled	0.363	14.50	0.96	50
Australia	milled	0.274	18.93	0.89	16
Crete	airborne	0.545	7.32	0.98	30
Dubai	sieved	0.391	13.04	0.96	35
Egypt	airborne	0.390	13.22	0.96	41
Great Basin	sieved	0.286	15.47	0.93	35
Peloponnese	airborne	0.535	6.84	0.95	17
Israel	sieved	0.477	10.11	0.91	39
Israel	milled	0.777	-1.43	0.95	13
Mojave	sieved	0.317	15.62	0.96	46
Morocco	milled	0.223	19.67	0.94	45
Namib	sieved	0.289	17.09	0.93	33
Taklamakan	sieved	0.355	15.00	0.93	21
Tenerife	airborne	0.455	10.16	0.97	14

Wilson et al. (2016) have shown that the biological material in the surface microlayer is probably an important source of atmospheric ice-nucleating particles (IN) that could influence cloud properties (Fig. 13a). They have found that organic material in the sea surface microlayer nucleates ice under conditions relevant for mixed-phase cloud and high-altitude ice cloud formation. The ice-nucleating material is probably biogenic and less than approximately 0.2 µm. They also studied exudates separated from cells of the marine diatom *Thalassiosira pseudonana* and found that they nucleate ice. These results suggested that organic material associated with phytoplankton cell exudates is a likely candidate for the observed ice-nucleating ability of the microlayer samples.

Global model simulations of marine organic aerosol (Fig. 13c), in combination with the measurements presented in Wilson et al. (2016), suggested that marine organic material may be an important source of ice-nucleating particles (INP) in remote marine environments such as the Southern Ocean, North Pacific Ocean and North Atlantic Ocean. Fig. 13b shows comparison of simulated INP with observations and indicates that although k-feldspar contribution to INP is significant, marine organics are major contributors to the levels of INP in the marine environment.

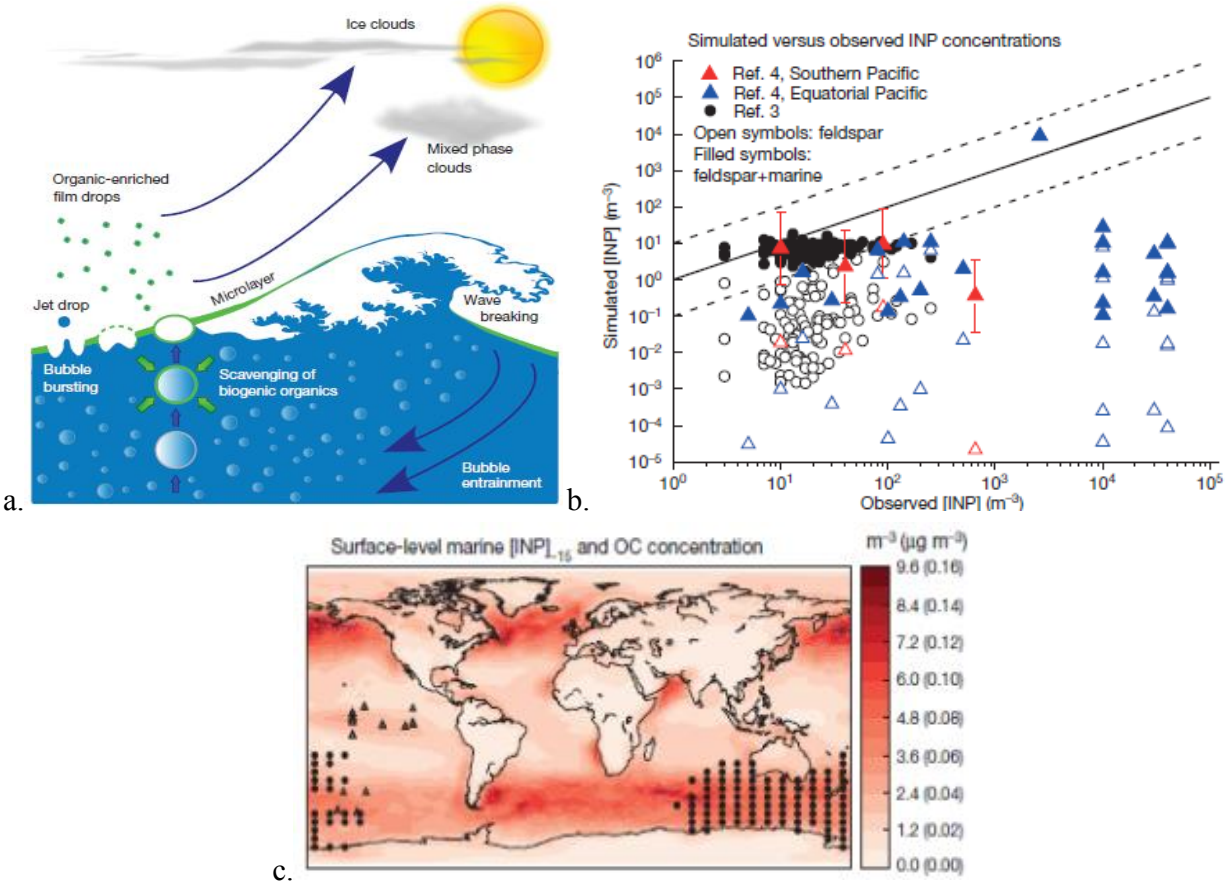

Figure 13. a) Sea-spray aerosol particles enriched in organic material are generated when bubbles burst at the air-sea interface. b) Comparison of simulated INP concentrations versus observations for the same location and at the activation temperature of the observations. Open symbols are for k-feldspar only and filled symbols are for mineral dust plus marine organics. c) Global simulated distribution of atmospheric marine biogenic IN (m^{-3}) active at -15°C

and surface-level marine organic aerosol mass concentration (μg m^{-3}). Figures are taken from Wilson et al. (Nature, 2016).

5. Uncertainty in global CCN and cloud droplet concentrations due to uncertainties in simulated OA using a global aerosol model

5.1. Singular model sensitivities

Exploratory global simulations have been performed using the chemistry/transport model TM4-ECPL that is able to simulate multiphase tropospheric chemistry accounting for volatile organic compounds chemistry as well as all major aerosol components, including secondary inorganic and organic aerosols (Kanakidou et al., 2012; Daskalakis et al., 2015). To facilitate sensitivity studies the model has been used in its low horizontal resolution of 6x4 in longitude and latitude and 34 vertical hybrid layers from the surface up to the 0.1 hPa pressure level.

Aerosol dynamics (nucleation, mixing and growth by condensation and coagulation) in the atmosphere are parameterized using the M7 microphysics model (Vignati et al., 2004) incorporated in TM4-ECPL. In the M7 model, particles are divided in the water-soluble particles (in nucleation, Aitken, accumulation and coarse mode) and in insoluble particles. Simulations have been performed using ECMWF (European Center for Medium – Range Weather Forecasts) Interim re–analysis project (ERA – Interim) meteorology (Dee et al., 2011). The results of the simulations for the years 2012 and 2013, size-resolved aerosol numbers and chemical composition for the stations of interest were stored hourly for post-processing to calculate CCN number concentrations. The calculation of the CCN concentrations was then performed based on the Petters model as explained in section 3 (Petters et al., 2007). The hygroscopicity parameters, κ, for the internally mixed aerosols were computed using the volume fraction weighted hygroscopic parameter of each component. Hygroscopicity parameters for individual aerosol components used for the base case calculations presented here are: 0.61 for sulfate particles, 1.28 for sea-salt, 0.227 for primary particulate organic matter (POM) and secondary organic aerosols (SOA), 0.0 for dust and black carbon.

In **Figure 14** the seasonal variations of CCNs at the surface computed by the model for SS=0.2% are shown for various stations. Fig 14c depicts the monthly mean variability of the CCN concentrations computed by the TM4-ECPL model using the hygroscopicity parameters that experimentally determined (kappa(observed)) via the analysis of observations at the studied locations where sufficient data are available for analysis and is presented in section 1.3 (Table 2). The model is able to capture the order of magnitude of the CCN levels observed at these stations as depicted in Fig. 14a with the highest discrepancies of about a factor of 5 found for JFJ. Note that this station is located at about 3578 m a.s.l. height which is expected not to be well represented in the large grid of the coarse resolution of the model that was used for these sensitivities. Fig. 14d shows model results using low κ values as reported in the caption of Fig. 14. The comparison of

these figures shows that the model is performing the best with regard to observed CCN levels and variability (Fig. 14a) when the observationally derived κ values are used to describe the hygroscopic behavior of the individual aerosol components. These figures (14b,c,d) also show that the sensitivity of the calculations of CCN concentrations on the chosen κ values depends on the location of the stations studied, i.e. on the aerosol composition.

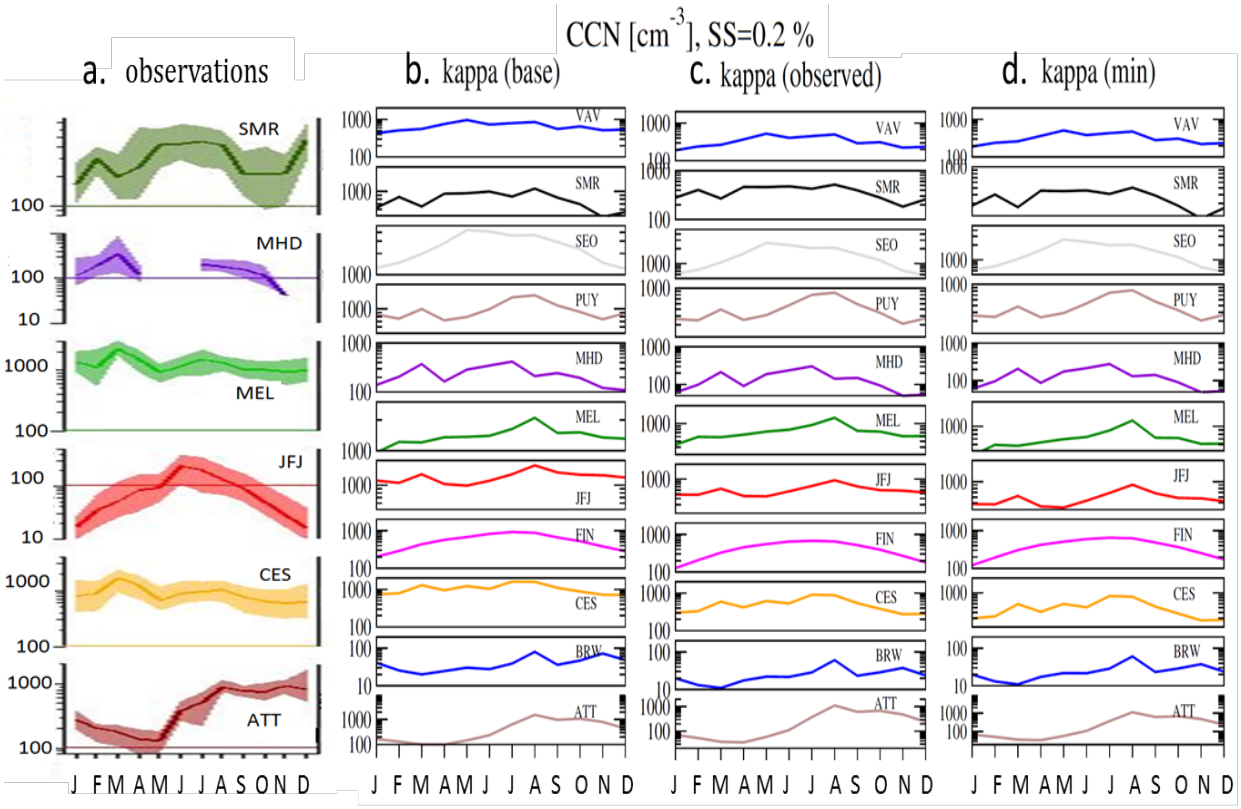

Figure 14. **Seasonal variations of CCNs for SS=0.2%** (a) from observations (section 1.2) and as calculated by TM4-ECPL for various stations and κ values for the individual components of aerosols (b) – kappa(base) - as listed above, (c) kappa(observed) as derived from observations and provided in Table 2; (d) kappa(min) calculated using κ(SO4)=0.61, κ(ss)=1.28 and κ(organics)=0.1.

Fig. 15 compares the observationally derived aerosol hygroscopic values (κ) and those calculated by the model for the different simulations as discussed above. As in the case of CCN concentrations, when the model uses the κ values of the individual components derived from observations, the hygroscopicity of the aerosol mixture (Fig. 15c) is computed to be close to that observed (Fig. 15a).

Except the simulations presented above, two additional global simulations have been performed: one neglecting the contribution of organic aerosol to the CCN formation (no organics) and one considering that the κ of organics is equal to zero (k_organics=0) (Fig. 16b,c).

When the hygroscopicity parameter of organics is assumed equal to zero then the presence of organics in the aerosols prohibits the CCN properties of the other aerosol components (Fig. 16b),

leading to significantly lower CCN levels than in the base case (Fig. 16a). On the opposite, in several cases, the absence of organics from the aerosol phase results in particles with higher hygroscopicity and thus better CCN properties (Fig 16c) than in the base case.

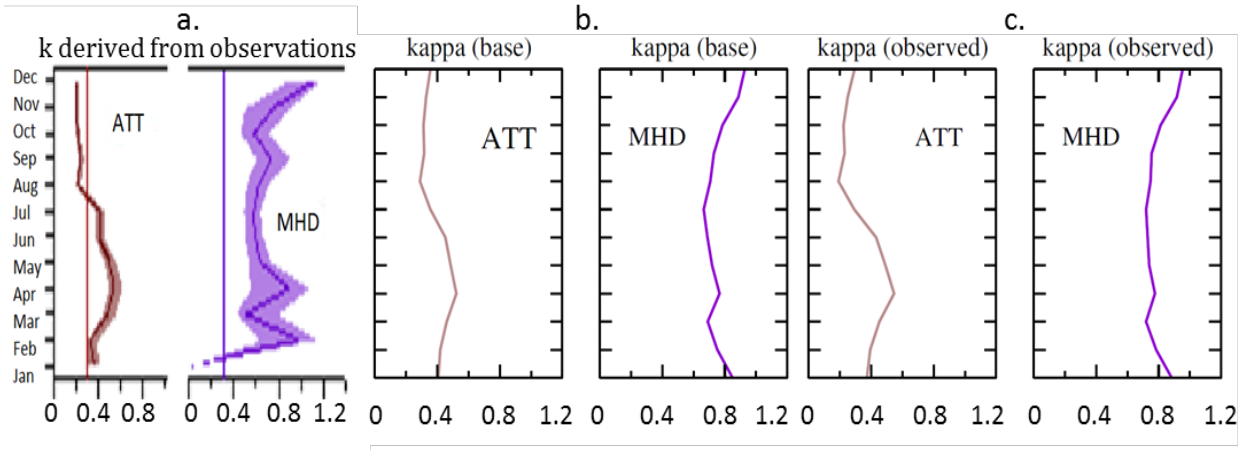

Figure 15. Seasonal variations of **hygroscopicity of aerosols (κ)** derived (a) from observations and as calculated by TM4-ECPL for various stations and using κ values for the individual components of aerosols (b) – kappa(base) - as listed in the model description, (c) kappa(observed) as derived from observations and provided in Table 2.

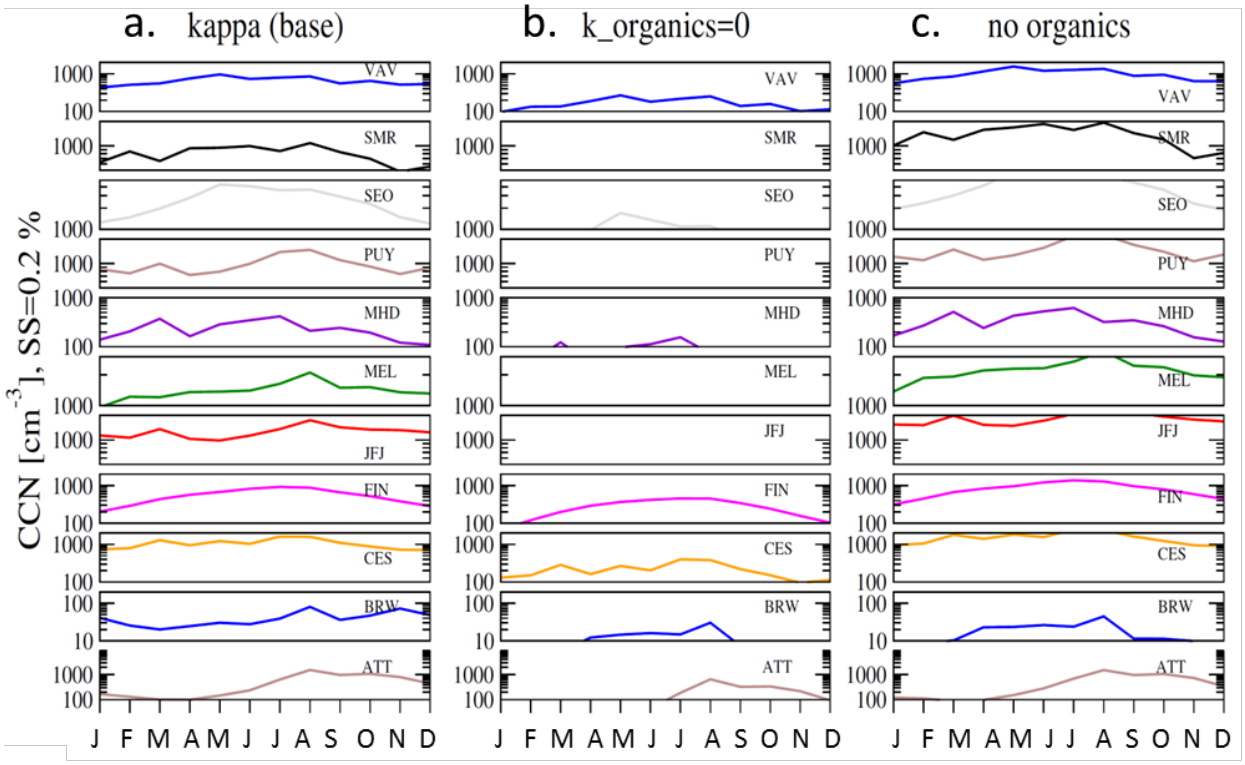

Figure 16. Seasonal variations of CCNs for SS=0.2% as calculated by TM4-ECPL for various stations (a) for the base case described above – kappa(base) ; (b) using k_organics=0; and (c) neglecting the presence of organics.

Furthermore, the impact of organics is different at the various stations due to the geographic variation in the contribution of organics to the aerosols, which is driven by emissions of aerosols and their precursors and ageing in the atmosphere. In Fig. 17a, the annual mean contribution of soluble organic aerosol (OA) components of anthropogenic origin to the total soluble OA at the surface is depicted.

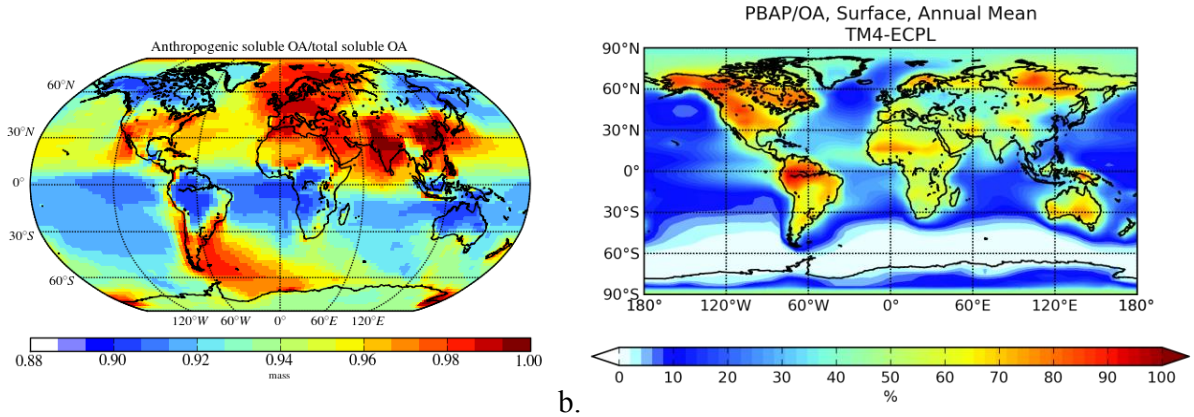

a. b.

Figure 17. (a) Annual mean mass contribution of soluble OA components of **anthropogenic origin** to the total soluble OA. (b) Contribution of primary biogenic particles (PBAP) of continental origin to OA at the surface as calculated by TM4-ECPL.

This contribution maximizes in the northern hemisphere over Central Europe, India and southeast China. Further global tropospheric simulations have been performed (Myriokefalitakis et al., EGU 2016a and Myriokefalitakis et al., 2016c) accounting for the contribution of primary biogenic particles to the organic aerosol component and this contribution was found to maximize in the tropics, although significant contribution is also calculated over North America and thee boreal forests (Fig.15b).

The sensitivities studies presented here are based on a number of selected simulations using one global model (TM4-ECPL) and show i) the importance of hygroscopicity parameters for the accurate representation of the observations, ii) that the presence of organics can be critical for the CCN properties of the particles, iii) that OA of anthropogenic origin is affecting CCN in most locations of the northern hemisphere while regions in the tropics be more affected by natural aerosols.

To consolidate these results and to investigate in addition the uncertainties in the computed aerosol size distribution that is important for the CCN computations as this has been evidenced by the analysis of observations in section 3, BACCHUS global model intercomparison has been initiated as described below.

5.2. BACCHUS global CCN modeling intercomparison exercise protocol

Objective: Consolidating the uncertainties estimate of the parameterizations of the impact of aerosol origin and chemistry in CCN

Specific objectives:
To evaluate model ability to simulate the spatial and temporal distribution of Cloud Condensation Nuclei (CCN) concentrations over a range of cloud-relevant supersaturations. Depending on the frequency and duration of the CCN datasets available, models will be assessed in terms of their ability to capture the observed:

1) Diurnal variation of CCN, aerosol number and chemical composition over selected areas and timeframes.
2) Daily and seasonal variation of CCN, aerosol number and chemical composition over selected areas and timeframes.
3) Persistence (autocorrelation) of CCN concentrations with time over selected regions.
4) Frequency distributions of CCN, aerosol number, hygroscopicity and vertical velocity.

Simulation period: 2012-2014 (3 years)

Time resolution of model results and observations: Hourly model results for selected stations and daily model results on global scale at surface to enable studies of the daily, weekly and monthly variations.

Hourly model output required *for the selected stations*:

1. Number concentration of aerosol larger than 40, 80, 120nm (dry diameter).
2. Aerosol hygroscopicity parameter at 40, 80, 120nm.
3. CCN concentration at 0.2% supersaturation for model to observations comparison.
4. CCN concentration at 0.1% supersaturation for model-to-model comparison.
5. CCN concentration at 0.6% supersaturation for model-to-model comparison.
6. Chemical composition of PM1 aerosols (SO4, organics (OM- all species together), BC, dust, sea-salt)

A supersaturation of 0.2% is selected for model to observations comparisons as the supersaturation is mostly available in CCN datasets. 0.1% and 0.6% are selected to evaluate simulated CCN spectra model divergence. The aerosol concentration and composition at different sizes allow for the construction of the CCN spectra for model/data evaluation wherever such data is available.

Locations for the comparison: Stations from ACTRIS database.

Nudging parameters for GCMs: wind, surface pressure, temperature (in order of importance).

MODEL DESCRIPTION:

1. Main model characteristics including model resolution and timestep, as well as the emissions used by the model.
2. Meteorological data used for CTMS and for nudging GCMs
3. Species specific κ used as input to the model.

FORMAT: Measurements: ascii or netcdf// model results: netcdf

The results of this model intercomparison are foreseen for the end of the year and will enable further evaluation of model uncertainties as part of the final deliverable of WP2.

6. References

Atkinson, J., Murray, B. J., Woodhouse, M. T., Whale, T. F., Baustian, K. J., Carslaw, K. S., Dobbie, S., O'Sullivan, D., and Malkin, T. L.: The importance of feldspar for ice nucleation by mineral dust in mixed-phase clouds, Nature, 498, 355 – 358, doi:10.1038/nature12278, 2013.

Boose, Y., Welti, A., Atkinson, J., Ramelli, F., Danielczok, A., Bingemer, H. G., Plötze, M., Sierau, B., Kanji, Z. A., and Lohmann, U.: Heterogeneous ice nucleation on dust particles sourced from 9 deserts worldwide – Part 1: Immersion freezing, Atmos. Chem. Phys. Discuss., doi:10.5194/acp-2016-438, in review, 2016.

Cappa, C. D. and Jimenez, J. L.: Quantitative estimates of the volatility of ambient organic aerosol, Atmos. Chem. Phys, 10, 5409–5424, doi:10.5194/acp-10-5409-2010, 2010.

Connolly, P., Topping, D. O., Malavelle, F., and McFiggans, G.: A parameterisation for the activation of cloud drops including the effects of semi-volatile organics, Atmos. Chem. Phys, 14, 2289–2302, doi:10.5194/acp-14-2289-2014, 2014.

Daskalakis, N., Myriokefalitakis, S., and Kanakidou, M.: Sensitivity of tropospheric loads and lifetimes of short lived pollutants to fire emissions, Atmos. Chem. Phys, 15, 3543–3563, doi:10.5194/acp-15-3543-2015, 2015.

Dee, D. P., Uppala, S. M., Simmons, A. J., Berrisford, P., Poli, P., Kobayashi, S., Andrae, U., Balmaseda, M. A., Balsamo, G., Bauer, P., Bechtold, P., Beljaars, A. C. M., van de Berg, L., Bidlot, J., Bormann, N., Delsol, C., Dragani, R., Fuentes, M., Geer, A. J., Haimberger, L., Healy, S. B., Hersbach, H., Hólm, E. V., Isaksen, L., Kållberg, P., Köhler, M., Matricardi, M., McNally, A. P., Monge-Sanz, B. M., Morcrette, J. J., Park, B. K., Peubey, C., de Rosnay, P., Tavolato, C., Thépaut, J. N., and Vitart, F.: The ERA-Interim reanalysis: configuration and performance of the data assimilation system, Q. J. Roy. Meteor. Soc., 137, 553-597, doi: 10.1002/qj.828, 2011.

Dusek, U., Frank, G. P., Hildebrandt, L., Curtius, J., Schneider, J., Walter, S., Chand, D., Drewnick, F., Hings, S., Jung, D., Borrmann, S., and Andreae, M. O.: Size matters more than chemistry for cloud-nucleating ability of aerosol particles, Science, 312, 1375-1378, doi:10.1126/science.1125261, 2006.

Fountoukis, C. and Nenes, A.: Continued development of a cloud droplet formation parameterization for global climate models, J. Geophys. Res., 110, D11212, doi:10.1029/2004JD005591, 2005.

Hermansson, E., Roldin, P., Rusanen, A., Mogensen, D., Kivekäs, N., Väänänen, R., Boy, M., and Swietlicki, E.: Biogenic SOA formation through gas-phase oxidation and gas-to-particle partitioning - a comparison between process models of varying compexity, Atmos. Chem. Phys, 14, 11 853 – 11 869, 2014.

Kanakidou, M., Duce, R. A., Prospero, J. M., Baker, A. R., Benitez-Nelson, C., Dentener, F. J., Hunter, K. A., Liss, P. S., Mahowald, N., Okin, G. S., Sarin, M., Tsigaridis, K., Uematsu, M., Zamora, L. M., and Zhu, T.: Atmospheric fluxes of organic N and P to the global ocean, Glob. Biogeochem. Cycles, 26, doi:10.1029/2011GB004277, GB3026, 2012.

Murray, B. J., Broadley, S. L.,Wilson, T.W., Atkinson, J. D., andWills, R. H.: Heterogeneous freezing of water droplets containing kaolinite particles, Atmos. Chem. Phys., 11, 4191 – 4207, doi:10.5194/acp-11-4191-2011, 2011.

Niemand, M., Möhler, O., Vogel, B., Vogel, H., Hoose, C., Connolly, P., Klein, H., Bingemer, H., DeMott, P., Skrotzki, J., and Leisner, T.: A particle-surface-area-based parameterization of immersion freezing on desert dust particles, J. Atmos. Sci., 69, 3077–3092, 2012.

Petters, M. D. and Kreidenweis, S. M.: A single parameter representation of hygroscopic growth and cloud condensation nucleus activity, Atmos. Chem. Phys., 7, 1961-1971, doi:10.5194/acp-7-1961-2007, 2007.

Van Dingenen, R., Raes, F., Putaud, J.-P., Baltensperger, U., Charron, A., Facchini, M.-C., Decesari, S., Fuzzi, S., Gehrig, R., Hansson, H.-C., Harrison, R., Hüglin, C., Jones, A., Laj, P., Lorbeer, G., Maenhaut, W., Palmgren, F., Querol, X., Rodriguez, S., Schneider, J., ten Brink, H., Tunved, P., Tørseth, K., Wehner, B., Weingartner, E., Wiedensohler, A., and Wåhlin, P.: A European aerosol phenomenology - 1: physical characteristics of particulate matter at kerbside, urban, rural and background sites in Europe, Atmos. Environ., 38, 2561 – 2577, doi:10.1016/j.atmosenv.2004.01.040, 2004

Rose, D., Nowak, A., Achtert, P., Wiedensohler, A., Hu, M., Shao, M., Zhang, Y., Andreae, M. O., and Pöschl, U.: Cloud condensation nuclei in polluted air and biomass burning smoke near the mega-city Guangzhou, China – Part 1: Size-resolved measurements and implications for the modeling of aerosol particle hygroscopicity and CCN activity, Atmos. Chem. Phys., 10, 3365-3383, doi:10.5194/acp-10-3365-2010, 2010.

7. Publications issued from the project

Conferences:

Fanourgakis G. S., S. Myriokefalitakis, and M. Kanakidou, Study of the CCN formation as a function of aerosol components: session AS4.5, EGU2016-3534, poster presentation, Vienna, 2016.

Myriokefalitakis S., G. Fanourgakis, and M. Kanakidou, The contribution of bioaerosols to the organic carbon mass of the atmosphere, session AS4.5, EGU2016-14209, oral presentation, Vienna, 2016a.

Myriokefalitakis S., A. Nenes, M. Kanakidou, Human-driven changes in dissolved phosphorus deposition to the ocean, session AS4.6, abstract EGU2016-3552, poster presentation, Vienna, 2016d.

Schmale et al., Overview on ACTRIS cloud condensation nuclei measurements results, EAC, Milano, 2015

Schmale et al., Synthesis of the ACTRIS Network Cloud Condensation Nuclei Measurements, AGU, San Francisco, 2015

Schmale et al., Cloud condensation nuclei closure study on long-term observation data,session AS4.5, EGU2016-8951, oral presentation, Vienna, 2016.

Schmale et al., Global synthesis of multi-year cloud condensation nuclei observations, IGAC, Beckenridge, 2016 (upcoming)

Papers:

Crooks, M., Connolly, P., Topping, D., and McFiggans, G.: The co-condensation of semi-volatile organics into multiple aerosol particle modes, Geosci. Model Dev. Discuss., doi:10.5194/gmd-2015-187, in review, 2016.

Myriokefalitakis S., Nenes A., Baker A.R., Mihalopoulos N., Kanakidou M.: Bioavailable atmospheric phosphorous supply to the global ocean: a 3-D global modelling study, submitted to Biogeoscience Discuss., bg-2016-215, 2016b.

Myriokefalitakis S., Fanourgakis G., Kanakidou M. The contribution of bioaerosols to the organic carbon of the atmosphere, in the Proceeding of the COMECAP 2016, Elsevier publications in press, 2016c

Wilson, T. W., Ladino, L. A., Alpert, P. A., Breckels, M. N., Brooks, I. M., Browse, J., Burrows, S. M., Carslaw, K. S., Huffman, J. A., Judd, C., Kilthau, W. P., Mason, R. H., McFiggans, G., Miller, L. A., Najera, J. J., Polishchuk, E., Rae, S., Schiller, C. L., Si, M., Temprado, J. V., Whale, T. F.,Wong, J. P. S.,Wurl, O., Yakobi-Hancock, J. D., Abbatt, J. P. D., Aller, J. Y., Bertram, A. K., Knopf, D. A., and Murray, B. J.: A marine biogenic source of atmospheric ice-nucleating particles, Nature, 525, 234–238, doi:10.1038/nature14986, 2015.

Papers in preparation with tentative titles:

"Synthesis of multi-year cloud condensation nuclei observations from 11 stations: Seasonal variability and closure studies"
J. Schmale, S. Henning, F. Stratmann, S. Decesari, J.S. Henzing, G.P.A. Kos, P. Schlag, R. Holzinger, P.P. Aalto, H. Keskinen, M. Paramonov, L. Poulain, K. Sellegri, J. Ovadnevaite, M. Krüger, S. Carbone, J. Brito, A. Jefferson, J. Whitehead, K. Carslaw, S.S. Yum, M. Park, A. Kristensson, R. Fröhlich, E. Herrmann, E. Hammer, G. Motos , N. Bukowiecki, A. Wiedensohler, A. Sonntag, W. Birmili, K.F.A. Frumau, A. Kiendler-Scharr, M. Äijälä, L. Heikkinen, T. Petäjä, M. Kulmala, D. Picard, C. O'Dowd, J. Bialek, C. Pöhlker, H. Su, U. Pöschl, M. Andreae, P. Artaxo, H. Barbosa, J. Ogren, G. McFiggans, E. Swietlicki, G. Frank, B. Svenningsson, C. Wittborn, A. Bougiatioti, N. Kalivitis, T. Nenes, N. Mihalopoulos, U. Baltensperger, M. Gysel (note the list of co-authors is not yet complete and not in the final order)

"A combined data set of global, multi-year cloud condensation nuclei number concentrations, aerosol size distribution and chemical composition observations – data descriptor "
J. Schmale, S. Henning, F. Stratmann, C. Reddington, K. Pringle, J.S. Henzing, G.P.A. Kos, P. Schlag, R. Holzinger, P.P. Aalto, H. Keskinen, M. Paramonov, L. Poulain, K. Sellegri, J. Ovadnevaite, M. Krüger, S. Carbone, J. Brito, A. Jefferson, J. Whitehead, K. Carslaw, S.S. Yum, M. Park, A. Kristensson, R. Fröhlich, E. Herrmann, E. Hammer, G. Motos , N. Bukowiecki, A. Wiedensohler, A. Sonntag, W. Birmili, K.F.A. Frumau A. Kiendler-Scharr, M. Äijälä, L. Heikkinen, T. Petäjä, M. Kulmala, D. Picard, C. O'Dowd, J. Bialek, C. Pöhlker, H. Su, U. Pöschl, M. Andreae, P. Artaxo, H. Barbosa, J. Ogren, G. McFiggans, E. Swietlicki, G. Frank, B. Svenningsson, C. Wittborn, A. Bougiatioti, N. Kalivitis, T. Nenes, N. Mihalopoulos, U. Baltensperger, M. Gysel (note the list of co-authors is not yet complete and not in the final order)